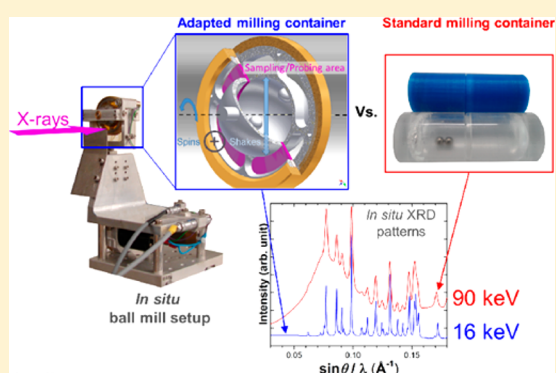


Innovative *in Situ* Ball Mill for X-ray DiffractionVoraksmý Ban,[†] Yolanda Sadikin,[‡] Michael Lange,[†] Nikolay Tumanov,^{§,||} Yaroslav Filinchuk,[§] Radovan Černý,[‡] and Nicola Casati^{*,†}[†]Swiss Light Source, Paul Scherrer Institut, 5232 Villigen PSI, Switzerland[‡]Laboratory of Crystallography, DQMP, University of Geneva, quai Ernest-Ansermet 24, 1211 Geneva, Switzerland[§]Institute of Condensed Matter and Nanosciences, Université catholique de Louvain, place L. Pasteur 1, 1348 Louvain-la-Neuve, Belgium^{||}Department of Chemistry, University of Namur, rue de Bruxelles 61, 5000 Namur, Belgium

Supporting Information

ABSTRACT: The renewed interest of mechanochemistry as an ecofriendly synthetic route has inspired original methodologies to probe reactions, with the aim to rationalize unknown mechanisms. Recently, Friščić *et al.* (*Nat. Chem.* 2013, 5, 66–73, DOI: 10.1038/nchem.1505) monitored the progress of milling reactions by synchrotron X-ray powder diffraction (XRPD). For the first time, it was possible to acquire directly information during a mechanochemical process. This new methodology is still in its early stages, and its development will definitively transform the fundamental understanding of mechanochemistry. A new type of *in situ* ball mill setup has been developed at the Materials Science beamline (Swiss Light Source, Paul Scherrer Institute, Switzerland). Its particular geometry, described here in detail, results in XRPD data displaying significantly lower background and much sharper Bragg peaks, which in turn allow more sophisticated analysis of mechanochemical processes, extending the limits of the technique.



Nowadays, *in situ* materials characterization techniques are extensively used, as they give an accurate description of a sample in a particular state. *In operando* measurements, on the other hand, are crucial as they allow one to probe continuously a dynamic state, such as the evolution of a process, without disrupting the process itself.

One category of such processes, where both *in situ* and *in operando* measurements are essential, is mechanochemical reactions. Mechanochemistry has attracted special attention as a promising alternative synthetic strategy to traditional “wet chemistry” methods.^{1,2} As a result, the most recent years have witnessed a rise of novel grinding methods, paving the way to novel reactions and/or improving the yield of a particular final product.³

Ball milling is a way to induce mechanochemical reactions: it involves “shaking” a container with powder reagents and hard (e.g., stainless steel) balls, which provides a transfer of kinetic energy from the container to the balls and from the balls to the powder mixture, resulting in reactivity. A large body of work exists on *ex situ* studies,^{4–6} where the materials are reacted and afterward analyzed, but they cannot describe transitional states, kinetics and dynamics during the mechanochemical reaction itself. This can instead be addressed by *in operando* measurements.

Up to now, available *in operando* measurements were mainly the monitoring of physical data during the milling reaction such

as recording of temperature or pressure.^{7–10} They provide some insights into the environmental conditions during the reaction but are not sufficient to describe precisely the chemical processes taking place inside the reactor. The latest state of the art is the real-time monitoring of mechanochemical reactions by X-ray powder diffraction (XRPD).¹¹ For the first time a mechanochemical reaction was monitored *in operando* by X-rays, yielding direct information on the phase evolution during the milling process. The data obtained were promising but insufficient for a comprehensive data analysis. For this reason, other techniques such as infrared or Raman spectroscopy^{12,13} are often required to bring complementary information to outline the reaction mechanisms.

However, as quick, efficient, and good the analytical instruments might be, the container design is often neglected and studies to date^{11,12} have been carried out with X-rays passing through its entire body. As powder from a large object is analyzed, these types of measurements result in broadened peaks that can include not only one but different phase peaks hindering data analysis (see Supporting Information Figure S1).

One of the most intuitive solutions to this problem is to reduce the part of the probing area for example by having a

Received: July 21, 2017

Accepted: November 13, 2017

Published: November 13, 2017

smaller volume specifically dedicated for analytical measurements. On the other hand, this simple idea would require several stringent criteria in order to be effective.

The container design has to address the following: (1) good sampling of the powder inside the milling chamber (efficient and fast exchange between the milling chamber and the collection area, which is important for a reaction and for obtaining the most credible picture possible while collecting data); (2) high quality of the experimental data (good signal-to-noise ratio improved by the path of the incident and outgoing beam probe through the vessel).

To realize these criteria, the grinding container may be connected to a separated “probing chamber” where the analysis is performed but the balls cannot access. As no ball impact is expected, in turn, the walls of the probing chamber can be thin and made of less mechanically robust material, such as plastic foil. With these lighter “probing windows”, less hard X-rays can then be used, further separating the peaks and increasing the cross-section with the sample. In a previous work,¹⁴ we demonstrated the efficiency of this two-part milling container concept by 3D printing several jar prototypes. This approach with a modest budget (*i.e.*, only investment in a 3D printer and cost of raw polymers) has provided data with a reduced background and improved angular resolution. The present work is a further development of this new generation of container tackling the difficulties we encountered previously.

Here, we describe such an innovative grinding-jar design, which improves the data quality collected during *in situ* XRPD ball milling and illustrate its benefits with different examples.

EXPERIMENTAL SECTION

Conditions of the Experiment. *In situ* ball milling experiments were performed at the X04SA Materials Science (MS) beamline¹⁵ at the Swiss Light Source (SLS), Paul Scherrer Institute. The ball mill setup was aligned with an X-ray camera such that the incident beam hits the window most of the time during the milling. The powder mixture was loaded in the jar with stainless steel balls in a ratio of 1:5 or 1:10 powder-to-ball. The ball mill device oscillations were set at 40 Hz.

The radiation beam was monochromatized to 16 or 17.5 keV. The exact wavelength was refined from the lattice parameters of Si 640d NIST standard.

During a typical *in situ* ball milling experiment, the X-ray beam passes through the probing windows while the jar is vigorously shaken and slowly spun. Scattered X-rays were detected with a 1D multistrip detector Mythen II or a 2D hybrid pixel array detector Pilatus 6M. The *in situ* ball milling layout at the beamline is shown in Figure S2.

In the Mythen configuration, the ball mill setup is placed at approximately 760 mm from the 1D detector. The primary X-ray beam was horizontally focused and slit down to 1 mm, while vertically it was fully focused to around 50 μm . The patterns are collected in a 2θ range of 0° – 40° with two detector positions for a typical time of 20 s (10 s per detector position) or in a fast mode acquisition with a fixed detector position. Data are postprocessed automatically after data acquisition.

In the 2D detector configuration, the setup is placed at approximately 885 mm from the area detector. The focused primary X-ray beam was slit down to obtain a square beam of about 0.8 mm^2 . Patterns were collected every 10 s in a shutterless operation mode. The readout time is shorter than 3 ms. The 2D images were calibrated from LaB₆ 660a NIST

standard and azimuthally integrated using the Dioptas program.¹⁶

All the XRPD patterns either from the Mythen II or Pilatus 6M detector presented in this work are plotted without any background correction.

Description of Ball Mill Setup. The setup is divided into three main parts: a device for vertical shaking, a holder, and a grinding container (Figure 1).

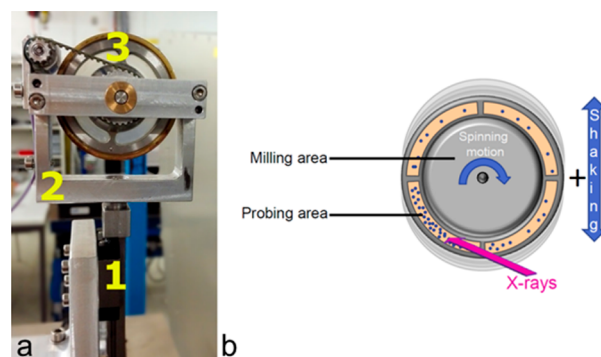


Figure 1. (a) Ball mill setup with (1) the shaking device, (2) frame holder, and (3) jar container; (b) schematic of the jar container and motion principles.

The innovative part is the grinding container, which consists of two metallic half-jars, a Teflon gasket, and a brass compression nut (Figure 2). Each half-jar has a hollow hemispherical central part where the milling is done, surrounded by a perforated circular part defining the probing chamber (Figure 2a). This probing chamber has four curved arc apertures (separated by four small pillars) covered by a thin plastic film (Figure 2b), and its depth is defined by the Teflon gasket (Figure 2c) intercalated between the two half-jars. On the outer part of each half-jar, there is a short rod at the hemisphere apex forming the rotation axis of the jar. A pinion gear is fixed on the rod of one of the half-jars. A system of pins and holes on each metallic part connects the two pieces together with the joint between. The entire vessel is then sealed manually by the compression nut (Figure 2d) and tightened with a dedicated wrench. Two sizes of grinding jar are available: a big one with a small probing area and a small one with a larger probing area. The grinding chamber volumes are, respectively, 17 and 9 cm^3 .

The holder is a rectangular frame with holes on both sides and a miniature motor positioned on the top of an edge (Figure 1a). The holder is screwed to the arm of the ball mill device. The jar fits into the holes of the holder by its rotation axis and is connected to the miniature motor through a toothed belt set on the pinion gear. Thus, the vessel can rotate continuously on its axis at a rate of 0.1–0.5 Hz.

The shaking device is either a modified PULVERISETTE 23 from Fritsch GmbH going up to 50 Hz or a homemade device going up to 80 Hz. Frequency of the milling and rotation speed of the jar can be remotely controlled to synchronize the experiment outside the hutch.

The setup is primarily used in a vertical mode (Figure S2); *i.e.*, the shaking is done vertically; however, horizontal shaking is also possible.

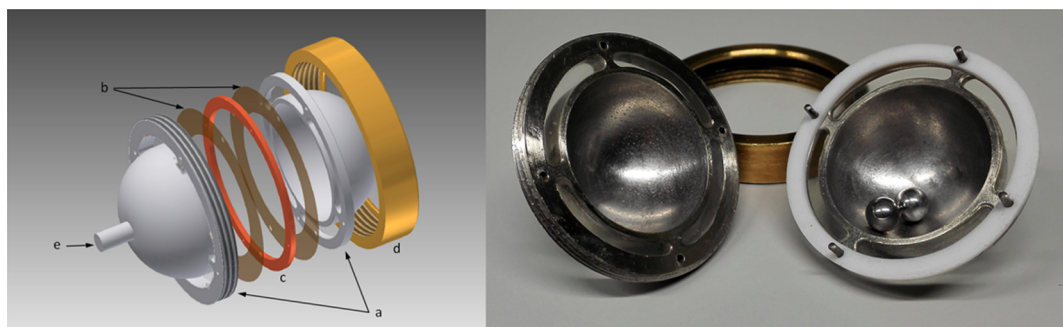


Figure 2. Technical drawing and picture of jar design piece by piece. It consists in two half-jars composed of a hollow half-spherical central part and a circular ring with four arc apertures (a), two sheets (b), a gasket (c), a compression nut (d), and the pinion (e).

RESULTS AND DISCUSSION

The first novelty of the grinding container is its two-part building, *i.e.*, a milling chamber surrounded by a continuous “probing” ring, such as a circular gutter, devoted to probing and sampling. The jar can be made entirely of the same material such as in Plexiglas (Figure S3a). However, the design allows more flexibility in the choice of materials: as balls cannot enter in the probing area, these two parts can be considered independently. On one hand, the milling part can be made of hard materials, such as stainless steel or even tungsten carbide, providing more energy during the ball impacts for the mechanochemical reactions than plastic materials. On the other hand, the groove can be made of more fragile material having a reduced absorption for X-rays such as Ultem or Kapton film (Figure S3b,c and Figure S4). The width of the probing volume can be adjusted by the thickness of the Teflon gasket. In the practical case of diffraction techniques, the smaller the width of the side chambers, the less broadening effect on Bragg peaks observed. This simple statement is supported by Figure 3, showing comparable full width at half-

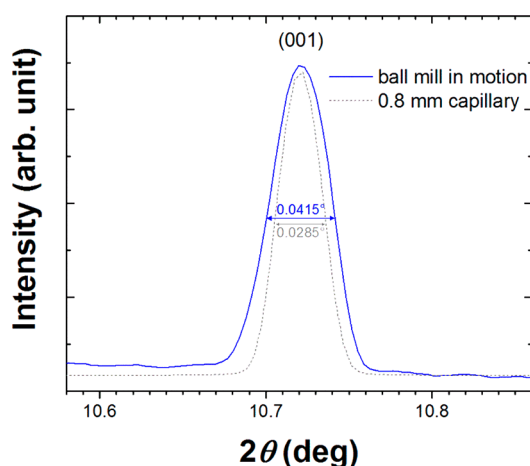


Figure 3. Comparison of fwhm of Bragg peak (001) of LaB_6 660a collected with Pilatus detector in a 0.8 mm diameter capillary (dashed line) and in the milling jar in motion (solid line). $\lambda = 0.776 \text{ \AA}$.

maximum (fwhm) for LaB_6 data collected in a 0.8 mm capillary and in our prototype in motion. This main improvement in the peak shape would not have been possible if the X-rays were passing through the entire jar.^{11,12} Moreover, the adapted jar is suitable for working with lower energy X-rays with the benefits of a larger scattering cross-section with the sample and, above all, to improve the XRPD pattern resolution. Both optimized

geometry and appropriate material of the probing chamber lead to data of higher quality than existing *in operando* ball mill setups.^{11,12} Data can be analyzed as is, without the need for any background subtraction (Figure 4); data quality is almost as

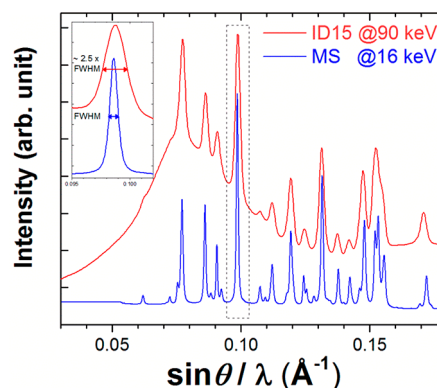


Figure 4. Comparison of the first *in situ* ball milling (red top curve) at ESRF ID15 beamline (Grenoble, France) versus optimized setup (blue bottom curve) at SLS MS beamline (Villigen, Switzerland) for the reaction between LiBH_4 and CsBH_4 .

good as that for a sample acquired in a capillary (Figure 3). Some diffraction from the pillars separating the probing area can be identified in the XRPD patterns, though their intensities are often negligible compared to the studied powder.

The second novelty is the dual motion during the milling that combines the normal vertical shaking and a continuous slow rotation of the jar (Figure 1b). In our previous prototypes (see Table S1), the powder tended to stick in the groove and thus the same powder portion was probed over time. The general shaking movement of 10 mm amplitude was not sufficient to push the powder out from the 7 mm groove. The additional slow spinning prevents this problem by bringing the powder to the top and allowing it to leave the probing area by a combination of shaking and gravity. The powder then re-enters the grinding chamber, thus maintaining a volumetrically homogeneous reaction. Moreover, any lateral wobbling during the motion, which would further contribute to the Bragg peak enlargement, is minimized thanks to our homemade ball mill (Figure S5).

The innovative part of the *in operando* ball mill setup derives from the specially engineered milling container. In the previous *in operando* ball mill setups,^{11,12} the principle flaws were the broad Bragg peaks. In addition to the dominant background observed in the diffraction patterns intrinsic to the jar, the diffraction of the milling balls could at times be stronger than

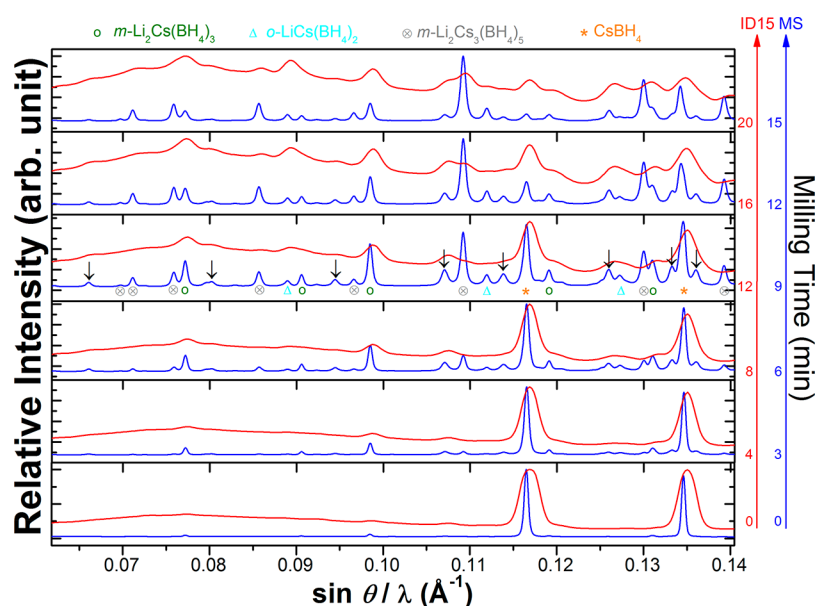


Figure 5. Comparison of XRPD patterns collected during the mechanochemical reaction between LiBH_4 and CsBH_4 , in red at ID15 (90 keV) and in blue at MS (16 keV). The black arrow markers (third pattern from the top) spot the unknown phase. Other peaks are marked in the same pattern to highlight the present phases.

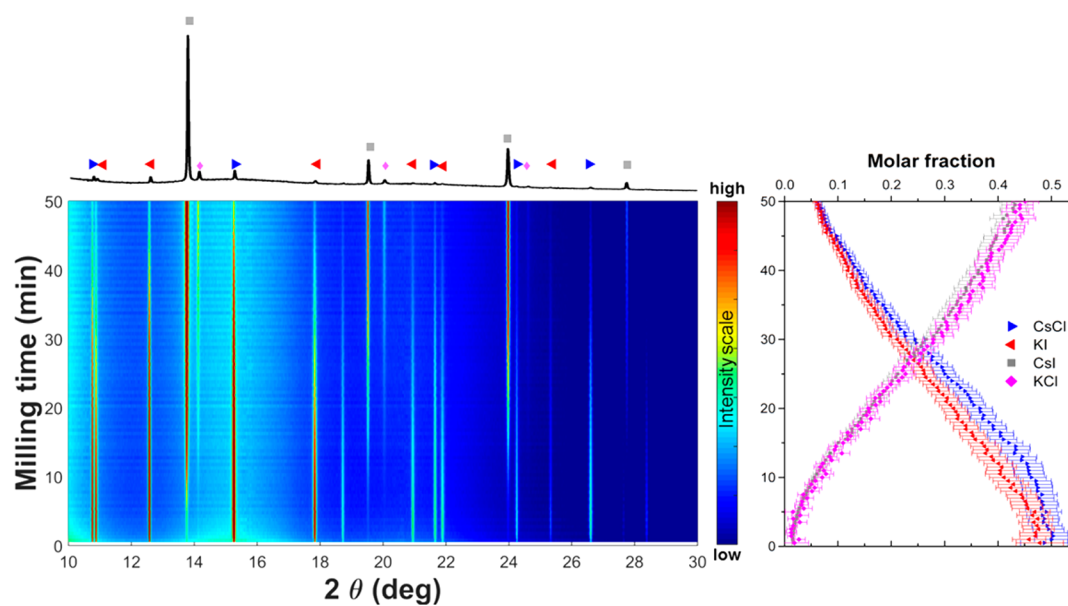


Figure 6. 2D projection of the time-resolved diffractograms (on the left) and Rietveld-extracted molar fraction (on the right) of the milling reaction between CsCl and KI . The last collected diffractogram at 50 min is plotted at the top of the left panel. $\lambda = 0.776 \text{ \AA}$. All diffractograms were collected with Mythen II detector.

that of the studied sample. The concept of the two-part building minimizes these artifacts. In the present report and in our previous work,¹⁴ however, the question of the powder sticking in the probing area was still a drawback of the device. With this in mind, the additional spinning motion of the jar was introduced, ensuring a continuous circulation of the powder from one chamber to the other.

There are some notable limitations to the device. While the powder is continuously refreshed, the minimum time for all of it to be recycled in the grinding jar is the time of a half-turn of the spinning slow motion, about 1 s, as is theoretically evident and also observed in practice on all the reactions analyzed. It is therefore not meaningful to probe processes at a faster frame

rate than this. A more severe limitation is that concerning liquid-assisted grinding, where a few drops of liquid are added to the grinding mixture to modify or accelerate the outcome of a milled reaction. In this latter case, powders might agglomerate and “cake” inside the milling chamber or, even worse, inside the probing area which will jeopardize *in operando* measurements. While smaller quantities of liquid can be tolerated and in some cases an anticaking agent could be used, we found until now no general rule and some reactions cannot be observed with this device. Nevertheless, the device is still relevant in the majority of cases.

In the next paragraphs we present some examples to illustrate the advantages of such a device.

Reaction Pathway and Identification of Intermediates. The specific jar combined with softer X-rays improves considerably the quality of XRPD data. The example shown in Figure 5 stresses the importance of a good signal-to-noise ratio to precisely identify the formation of intermediates during a reaction. The example presents the formation of double cation borohydrides in the ball milled mixture of LiBH_4 and CsBH_4 showing a rich phase diagram.¹⁷ The figure displays the *in situ* ball milling performed with different ball mill setups at ID15 at the ESRF, Grenoble, France,¹⁸ and at MS (this work) collected every 12 s by a PerkinElmer detector and every 20 s by a Pilatus 6M, respectively.

In both cases during the initial stage of the reaction, the formation of a honeycomb-like $m\text{-Li}_2\text{Cs}(\text{BH}_4)_3$ phase is observed together with one unidentified phase. The analysis of the reaction pathways starts then to be more complicated as more phases appear. Indeed, with the original setup, a few Bragg peaks (in red curves) were either hidden under the high background produced by the milling jar itself or were overlapped under broad diffraction peaks from the size of the entire jar. It becomes challenging with this setup design to differentiate the formation of $m\text{-Li}_2\text{Cs}_3(\text{BH}_4)_5$ from $m\text{-Li}_2\text{Cs}(\text{BH}_4)_3$ or to clearly distinguish the appearance of the $o\text{-LiCs}(\text{BH}_4)_2$ phase. Our innovative grinding-container geometry produces much more detailed diffraction patterns as shown in the blue curves of Figure 5. Despite this, unequivocal indexing from the unknown phase could not be confirmed, due to the low molar fraction and the low symmetry typical of these systems.

Phase Quantification. Since the development of *in situ* ball milling, it has been possible to access previously unavailable data such as quantifying the different phases at a specific moment of the reaction pathway.^{11,19,20} This information is relevant to understand the reaction progress and thus a step forward toward the full understanding of mechanistic and kinetic details. The example presented is a simple exchange reaction between CsCl and KI (Figure 6) milled in a jar made in Plexiglas (Figure S3a). This reaction was chosen as it involves simple reagents with good scattering strength and a straightforward process, easy to detect and to follow. The data collection was done by the Mythen detector with each XRPD pattern taken every 20 s with two detector positions.

The phase quantification of the reagents and products were extracted from Rietveld analysis and then converted into molar fractions as shown in the 2D projection in Figure 6. At the beginning of the milling, the evolution of molar fractions slowly accelerates as the powders experience a significant comminution from the first ball impacts. Then a monotonous increase of the products and decrease of the reagents can be observed. In comparison with a reaction in liquid, where mixing is fast and reagents come in contact typically at a high repetition rate, the observed rate of this solid–solid reaction is rather linear as reactivity is strongly correlated to the accumulated number of ball impacts. This trend is attested by the smooth variation of the extracted molar fractions (Figure 6) and further demonstrates the uniform sample distribution throughout the milling thanks to the dual motion of the jar.

Measurements were done without any internal standard; *i.e.*, no amorphous phase was taken into account for the refinement, although a small fraction is probably present.

Line-Profile Analysis. The last example shows another kind of information that can be extracted from *in situ* XRPD patterns, namely, through line-profile analysis (Figure 7). By

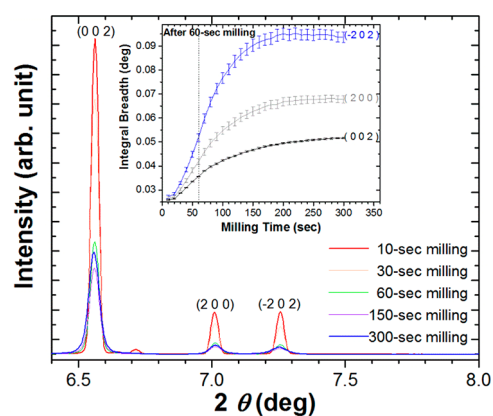


Figure 7. Bragg peaks evolution of vanillin over milling time. The insert describes the integral breadth evolutions of (002), (200), and (−202) reflections over milling time and the percentage of the integral breadth increase after 60 s of milling. $\lambda = 0.776 \text{ \AA}$.

monitoring the milling of a single compound, here vanillin in a stainless steel jar (Figure S3b), different behavior of Bragg peaks are observed from data collected every 10 s with a Pilatus 2D detector. Although we can monitor the effect of the balls grinding the powder, as shown with the vanillin milled over time (Figure 7), a quantitative description in dynamic conditions (state of the powder is in constant evolution and motion) is clearly more complex than in standard static measurements. However, the quality of the data with our setup is so significantly improved to permit a meaningful semi-quantitative description, for example, the integral breadth of each Bragg peak can be reliably extracted and corrected from the instrumental resolution, as seen in the inset of Figure 7. Each individual Bragg peak was refined separately and led to rather different results after subtraction of the instrumental contribution, even when close in scattering angle. The anisotropic response of powder diffraction peaks to grinding can quickly highlight the most fragile crystalline directions, likely to be related to defect generation and reactivity.

CONCLUSION AND PERSPECTIVES

There remains a long way to understand all the fundamental aspects of mechanochemical processes. Since the introduction of a new methodology developed by Friščić *et al.*^{11,21} a few years ago, there has been a renewed interest in unlocking the mechanisms of mechanochemical reactions as it was finally possible to access some evidence during the milling itself. Different features or analytical techniques^{12,13,20,22} were used in addition, providing complementary information on the ongoing process. However, in the past 5 years, no real improvements on the original setup were made. The *in operando* ball mill setup for XRPD presented here is designed for that purpose. As demonstrated by the examples described above, this novel design improves the collected XRPD patterns by drastically reducing the high background, predominant with the former milling cells,^{12,21} and by producing sharper Bragg peaks, revealing previously hidden features. This results in simplified data treatment with no loss of information. The two detectors available at the MS beamline are complementary in nature: the Pilatus 6M 2D detector gives more counting and particle statistics whereas the multistrip detector, Mythen II, has higher angular resolution which helps indexing and solving unknown phases. For this latter, once an unknown product is detected,

stopping the acquisition to obtain the highest quality data can also be considered as an option.

The extra spinning motion of the milling jar is also a big improvement. With the previous setups, shown in Table S1 and in our previous work,¹⁴ powder could be trapped inside the probing area, biasing the true reaction progress as the same part was probed over time. This cannot occur with the present prototype. Some developments around the setup are already in progress: heating up to 150 °C is already possible by positioning a cryojet directly on the milling jar, whereas cooling below 0 °C needs modifications to prevent ice formation on the window.

All these advances open up new perspectives such as the structure solution of reaction intermediates or the exact role of comminution and the defect development in the reactivity. It is worth noting that neither the efficiency of energy transfer nor the applied stress is the same from one milling device to another. Indeed, different types of stress are involved in a planetary ball mill than in a shaker mill. For this reason it is important to develop, in the future, other kind of mills for *in situ* measurement to precisely reproduce the reactional environment. Comminution processes generated by different sources of stress²³ (by impact, shearing, and friction, *etc.*) cannot be put aside and are important parts of the puzzle for deciphering mechanochemical mechanisms. Systematic studies are needed on this side and can be the key to explain the reproducibility or not of a reaction.

The *in operando* ball mill setup has been offered to the research community since September 2016 at MS beamline (SLS, Switzerland).

■ ASSOCIATED CONTENT

Supporting Information

The Supporting Information is available free of charge on the ACS Publications website at DOI: 10.1021/acs.analchem.7b02871.

Scheme describing the effect of the sample thickness on the diffraction peaks broadening, layout of the *in situ* ball milling at MS beamline, pictures of milling jars in different materials and of homemade *in situ* ball mill, diffraction patterns of the different plastic films, and table showing the different “simple groove” prototypes (PDF)

■ AUTHOR INFORMATION

Corresponding Author

*E-mail: nicola.casati@psi.ch.

ORCID

Voraksmý Ban: 0000-0002-8820-503X

Radovan Černý: 0000-0002-9847-4372

Nicola Casati: 0000-0002-4206-9239

Notes

The authors declare no competing financial interest.

■ ACKNOWLEDGMENTS

The research leading to these results has received funding from the European Community's Seventh Framework Program (FP7/2007-2013) under Grant Agreement No. 290605 (COFUND: PSI-FELLOW) and was partly supported by FNRS (Grant No. PDR T.0169.13).

■ REFERENCES

- (1) James, S. L.; Adams, C. J.; Bolm, C.; Braga, D.; Collier, P.; Friscic, T.; Grepioni, F.; Harris, K. D. M.; Hyett, G.; Jones, W.; Krebs, A.; Mack, J.; Maini, L.; Orpen, A. G.; Parkin, I. P.; Shearouse, W. C.; Steed, J. W.; Waddell, D. C. *Chem. Soc. Rev.* **2012**, *41*, 413–447.
- (2) Boldyreva, E. *Chem. Soc. Rev.* **2013**, *42*, 7719–7738.
- (3) Friscic, T. *J. Mater. Chem.* **2010**, *20*, 7599–7605.
- (4) Balaz, P.; Achimovicova, M.; Balaz, M.; Billik, P.; Cherkezova-Zheleva, Z.; Criado, J. M.; Delogu, F.; Dutkova, E.; Gaffet, E.; Gotor, F. J.; Kumar, R.; Mitov, I.; Rojac, T.; Senna, M.; Streletskii, A.; Wiecezok-Ciurawa, K. *Chem. Soc. Rev.* **2013**, *42*, 7571–7637.
- (5) Sepelak, V.; Duvel, A.; Wilkening, M.; Becker, K.-D.; Heitjans, P. *Chem. Soc. Rev.* **2013**, *42*, 7507–7520.
- (6) Ma, X.; Yuan, W.; Bell, S. E. J.; James, S. L. *Chem. Commun.* **2014**, *50*, 1585–1587.
- (7) Bellosa von Colbe, J. M.; Felderhoff, M.; Bogdanovic, B.; Schuth, F.; Weidenthaler, C. *Chem. Commun.* **2005**, 4732–4734.
- (8) Doppiu, S.; Schultz, L.; Gutfleisch, O. *J. Alloys Compd.* **2007**, *427*, 204–208.
- (9) Zhang, J.; Cuevas, F.; Zaidi, W.; Bonnet, J.-P.; Aymard, L.; Bobet, J.-L.; Lacroche, M. *J. Phys. Chem. C* **2011**, *115*, 4971–4979.
- (10) Jaques, B. J.; Osterberg, D. D.; Alanko, G. A.; Tamrakar, S.; Smith, C. R.; Hurley, M. F.; Butt, D. P. *J. Alloys Compd.* **2015**, *619*, 253–261.
- (11) Friščić, T.; Halasz, I.; Beldon, P. J.; Belenguer, A. M.; Adams, F.; Kimber, S. A. J.; Honkimäki, V.; Dinnebier, R. E. *Nat. Chem.* **2013**, *5*, 66–73.
- (12) Batzdorf, L.; Fischer, F.; Wilke, M.; Wenzel, K.-J.; Emmerling, F. *Angew. Chem., Int. Ed.* **2015**, *54*, 1799–1802.
- (13) Gracin, D.; Štrukil, V.; Friščić, T.; Halasz, I.; Užarević, K. *Angew. Chem., Int. Ed.* **2014**, *53*, 6193–6197.
- (14) Tumanov, N.; Ban, V.; Poulain, A.; Filinchuk, Y. *J. Appl. Crystallogr.* **2017**, *50*, 994–999.
- (15) Willmott, P. R.; Meister, D.; Leake, S. J.; Lange, M.; Bergamaschi, A.; Boge, M.; Calvi, M.; Cancellieri, C.; Casati, N.; Cervellino, A.; Chen, Q.; David, C.; Flechsig, U.; Gozzo, F.; Henrich, B.; Jaggi-Spielmann, S.; Jakob, B.; Kalichava, I.; Karvinen, P.; Krempasky, J.; Ludeke, A.; Luscher, R.; Maag, S.; Quitmann, C.; Reinle-Schmitt, M. L.; Schmidt, T.; Schmitt, B.; Streun, A.; Vartiainen, I.; Vitins, M.; Wang, X.; Wulschleger, R. *J. Synchrotron Radiat.* **2013**, *20*, 667–682.
- (16) Prescher, C.; Prakapenka, V. B. *High Pressure Res.* **2015**, *35*, 223–230.
- (17) Schouwink, P.; Smrcok, L.; Černý, R. *Acta Crystallogr., Sect. B: Struct. Sci., Cryst. Eng. Mater.* **2014**, *70*, 871–878.
- (18) Sadikin, Y. Novel solid electrolytes based on borohydrides and higher boranes. Ph.D. Thesis, No. 4963, Université de Genève, Geneva, Switzerland, 2016.
- (19) Halasz, I.; Friscic, T.; Kimber, S. A. J.; Užarevic, K.; Puskaric, A.; Mottillo, C.; Julien, P.; Strukil, V.; Honkimaki, V.; Dinnebier, R. E. *Faraday Discuss.* **2014**, *170*, 203–221.
- (20) Fischer, F.; Wenzel, K.-J.; Rademann, K.; Emmerling, F. *Phys. Chem. Chem. Phys.* **2016**, *18*, 23320–23325.
- (21) Halasz, I.; Kimber, S. A. J.; Beldon, P. J.; Belenguer, A. M.; Adams, F.; Honkimäki, V.; Nightingale, R. C.; Dinnebier, R. E.; Friščić, T. *Nat. Protoc.* **2013**, *8*, 1718–1729.
- (22) Užarević, K.; Štrukil, V.; Mottillo, C.; Julien, P. A.; Puškarić, A.; Friščić, T.; Halasz, I. *Cryst. Growth Des.* **2016**, *16*, 2342–2347.
- (23) Rumpf, H. *Chem. Ing. Tech.* **1965**, *37*, 187–202.